Interactions of the fatty acid-binding protein ReP1-NCXSQ with lipid membranes. Influence of the membrane electric field on binding and orientation

Vanesa V. Galassi [a], Marcos A. Villarreal [b], Velia Posada [a], Guillermo G. Montich [a,*]

[a] *Centro de Investigaciones en Química Biológica de Córdoba (CIQUIBIC), CONICET, Departamento de Química Biológica, Facultad de Ciencias Químicas, Universidad Nacional de Córdoba, Ciudad Universitaria, X5000HUA, Córdoba, Argentina*
[b] *Instituto de Investigaciones en Físico-Química de Córdoba (INFIQC), CONICET, Departamento de Matemática y Física, Facultad de Ciencias Químicas, Universidad Nacional de Córdoba, Ciudad Universitaria, X5000HUA, Córdoba, Argentina*

ARTICLE INFO

ABSTRACT

The regulatory protein of the squid nerve sodium calcium exchanger (ReP1-NCXSQ) is a 15 kDa soluble, intracellular protein that regulates the activity of the Na^+/Ca^{2+} exchanger in the squid axon. It is a member of the cellular retinoic acid-binding proteins family and the fatty acid-binding proteins superfamily. It is composed of ten beta strands defining an inner cavity and a domain of two short alpha helix segments. In this work, we studied the binding and orientation of ReP1-NCXSQ in anionic and zwitterionic lipid membranes using molecular dynamics (MD) simulations. Binding to lipid membranes was also measured by filtration binding assay. ReP1-NCXSQ acquired an orientation in the anionic membranes with the positive end of the macrodipole pointing to the lipid membrane. Potential of mean force calculations, in agreement with experimental measurements, showed that the binding to the anionic interfaces in low ionic strength was stronger than the binding to anionic interfaces in high ionic strength or to zwitterionic membranes. The results of MD showed that the electrostatic binding can be mediated not only by defined patches or domains of basic residues but also by a global asymmetric distribution of charges. A combination of dipole–electric field interaction and local interactions determined the orientation of ReP1-NCXSQ in the interface.

© 2013 Elsevier B.V. All rights reserved.

1. Introduction

In several examples, peripheral membrane proteins and soluble proteins that interact with lipid membranes have a defined orientation in the interface [1–9]. Specific lipid–protein interactions and nonspecific electrostatic interactions are the forces involved in determining the protein orientation in the interface. In some cases, it can be identified clusters or domains of basic residues in the protein that drive the interaction with anionic lipids [3,10–12]. On the other hand, evaluation of electrostatic potential by solving the Poisson–Boltzmann equation reveals that the microscopic shape together with the charge distribution in the protein topology determine the domains of defined polarity even when it is not obvious from the distribution of the ionizable residues

[13]. In line with this observation, it was described that fatty acid binding-proteins (FABPs) bind and acquire an orientation within the lipid membrane interface according to the global distribution of partial charges and to the profile of the electrostatic potential [14–16]. Electrostatic interactions also have a role in coupling the process of binding to the conformational changes in the interface. We found that the fatty acid binding-protein L-BABP binds to anionic lipid membranes acquiring either a native or a partly unfolded state. The extent of the conformational change correlates with the intensity of the electrostatic membrane surface potential [17]. In other few cases, it was found that conformational changes in proteins are directly related to the membrane electrostatic potential [18,19].

In this work we used ReP1-NCXSQ as an experimental model system to further study how electrostatic interactions, particularly those between the protein electric macrodipole and the membrane electric field, define the strength of binding and orientation of proteins in the membrane interface. ReP1-NCXSQ is an acidic protein that regulates the activity of the Na^+/Ca^{2+} exchanger in squid axon [20–23]. ReP1-NCXSQ belongs to the family of the cellular retinoic acid-binding protein (CRABP) and to the superfamily of FABPs. The structure, shown in Fig. 1A, is a flattened barrel composed of two orthogonal β-sheets delimiting an inner cavity and a domain composed of two α-helix segments (PDB ID: 3PPT, [23]). Fig. 1B shows the positively charged,

Lys and Arg, and the negatively charged Glu and Asp residues. The electrostatic isopotential surface at $+1$ and -1 mV and the electric macrodipole of ReP1-NCXSQ are shown in Fig. 1C.

The positive end of the macrodipole points towards the α-helix domain, which is in the opposite direction to the previously studied L-BABP [14]. Then, this is a very convenient experimental system to study the influence of the protein macrodipole in the binding strength and orientation in the lipid membrane.

First we measured the binding to large unilamellar vesicles (LUVs) of zwitterionic and anionic lipids. We found that electrostatics is a relevant force for membrane binding. Then we performed molecular dynamics (MD) simulations of ReP1-NCXSQ in anionic and zwitterionic membrane systems and calculated the potential of mean force (PMF) with distance-constrained simulations. The results show that the interactions of the protein macrodipole with the membrane electric field are relevant to determine the protein binding and orientation.

2. Materials and methods

2.1. Materials

ReP1-NCXSQ cDNA was synthesized and codon-optimized for *Eschericia coli*. 1-1-palmitoyl-2-oleoyl-*sn*-glycero-3-phosphoglycerol sodium salt (POPG) and 1-palmitoyl-2-oleoyl-*sn*-glycero-3-phosphocholine (POPC) were from Avanti Polar Lipids (Alabaster, AL). Amicon Ultra-0.5, Ultracel-100 Membrane concentrators were from EMD Millipore

2.2. Expression and purification of ReP1-NCXSQ

The cDNA for ReP1-NCXSQ was cloned into the expression vector pGEX4T2 and expressed in *E. coli* strain BL21. The fusion protein GST-ReP1-NCXSQ was purified by affinity chromatography in glutathione–sepharose resin and eluted with reduced glutathione. GST-ReP1-NCXSQ was cleaved with thrombin and ReP1-NCXSQ was purified by exclusion chromatography in Superdex 75. The ReP1-NCXSQ preparation produced a single band with an apparent MW = 15 kDa in SDS-PAGE. The protein was quantified by the absorbance at 280 nm using $\varepsilon_{280} = 14000$ M^{-1} cm^{-1}.

2.3. Large unilamellar vesicle preparation

LUVs were prepared as in Nolan et al. [24]. Pure phospholipids were dissolved in chloroform:methanol 2:1 vol:vol and dried as a thin film in a glass tube. The dry lipids were hydrated with unbuffered solutions of NaCl. After five cycles of freeze in liquid nitrogen and thaw at 30 °C, LUVs were prepared by ten cycles of extrusion through policarbonate filters with pores of 100 nm diameter. Dynamic light scattering measurements showed that the vesicles were of 96 nm with a size distrubution of ±7 (standard deviation) nm.

2.4. Filtration binding assay

Samples containing pure protein and lipid–protein mixtures were preincubated for 30 min at 22 °C, loaded in the upper chamber of Amicon concentrators with cutoff filter of 100 kDa, and spun down at 7000 ×*g* at 22 °C until 80% of the initial volume was eluted. The protein concentration was quantified in the initial sample and in the eluted fraction. After centrifugation, LUVs, together with membrane bound-protein, are retained in the upper chamber. Free ReP1-NCXSQ can cross the filter membrane. The concentration of protein in the eluant is equal to the concentration of free protein in equilibrium with membrane-bound protein. Lipid was not detected in the eluted material. pH of the lipid–protein mixtures was 6.7.

2.5. Molecular dynamics simulations

The protein structure was obtained from the X-ray crystallography (PDB ID: 3PPT) [23]. The simulation system (Fig. 2) was a triclinic cell of 7 nm in *x* and *y* directions, (this is the face where the membrane plane was located), and 10 nm in the *z* direction. The boxes contained one protein molecule, 128 molecules of POPG or POPC and 10,000 water molecules. The simple point charge water model SPC was used [25]. Coordinates for lipid membranes were from Kukol [26], available in www.gromacs.org/Downloads/User_contributions/Molecule_topologies/LipidsForGro96_53a6.zip. Membranes were pre-equilibrated for 50 ns before introducing the protein. In the "low ionic strength" systems, Na$^+$ ions were added as required to neutralize the lipid and protein negative charges (129 Na$^+$ ions for POPG and 1 Na$^+$ ion for POPC system). In the "high ionic strength" systems, extra Na$^+$ and Cl$^-$ ions were added randomly to obtain a concentration of 1 M NaCl in the unconstrained simulations and 0.5 M NaCl in the distance-constrained simulations used to calculate the PMF (168 Cl$^-$ ions and 297 Na$^+$ ions). The GROMOS96 force field with the G53A6 set of parameters [27] was used for the protein and the parameters described by Kukol [26] for the lipids. The charges on the amino acid side chains were according to the pKa estimated by the PROPKA web server [28], resulting in a negatively charged protein with a net charge $Z = -1$. Settings for MD were as in Villarreal et al. [14]. The electrostatic interactions were handled with the SPME version of the Ewald sums [29]. The settings
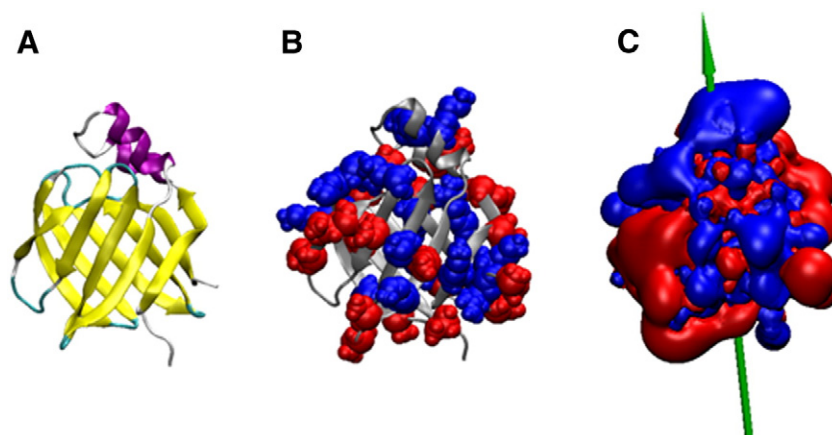

Fig. 1. The structure of ReP1-NCXSQ. A: colors are according to secondary structure. B: positively charged Lys and Arg residues are shown in blue, negatively charged Glu and Asp residues are shown in red. C: electrostatic isopotential surfaces at $+1$ mV are shown in blue and at -1 mV in red. The direction of the global macrodipole is also shown.
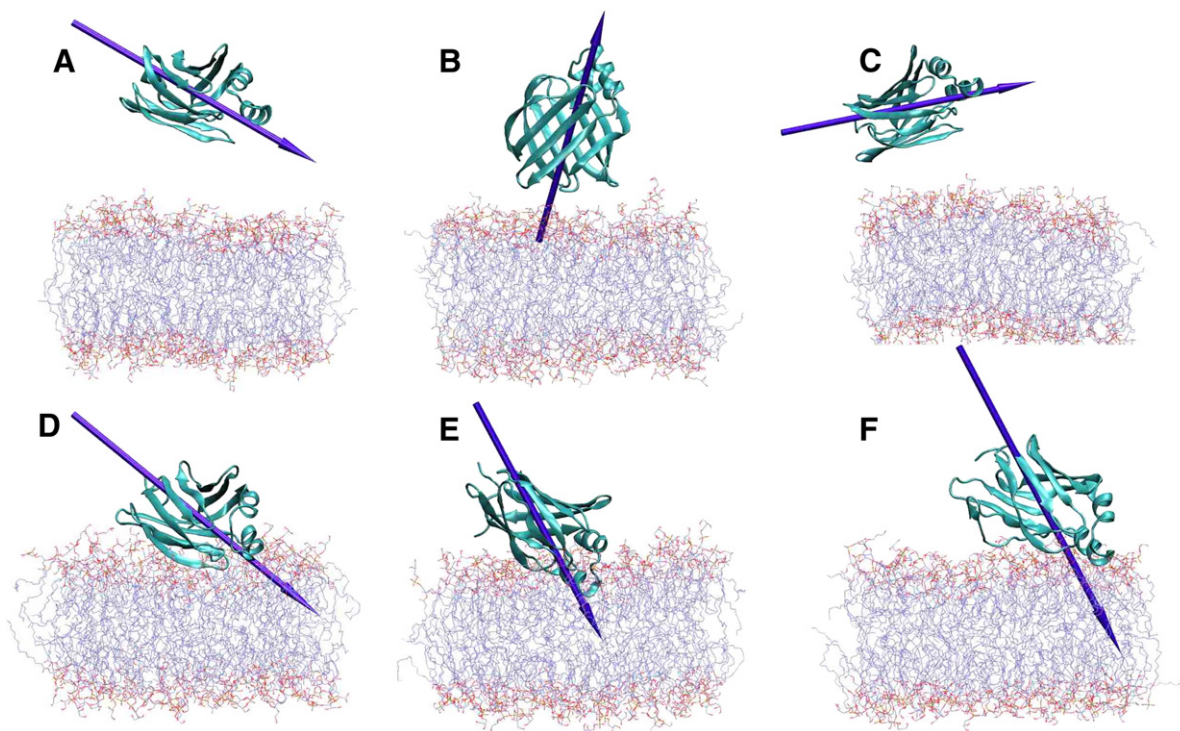
Fig. 2. Snapshots of the MD simulations of ReP1-NCXSQ in POPG membranes. A, B and C: initial frames for three different simulations. D, E and F: the corresponding simulations after 100 ns. Simulations were in low ionic strength. The arrows represent the protein electric macrodipole.

for the SPME method were as follows: a real space cutoff of 0.9 nm, a grid spacing of 0.12 nm, and a quartic interpolation. In all the simulations, a dielectric permittivity of 1 was assumed and the van der Waals interactions were cut off at 1.4 nm. The simulations were carried out in the NPT ensemble using the v-rescale thermostat and Berendsen barostat [30]. The protein, the membrane, and the solvent were weakly coupled separately to a temperature bath with a reference temperature of 320 K and a relaxation constant of 0.2 ps. This temperature was used to increase sampling and help reaching convergence, and to ensure a fluid state in lipid membranes. The pressure was maintained constant by coupling to a reference pressure of 1 bar with a relaxation constant of 2.0 ps and a compressibility of 5×10^{-5} bar^{-1}. Dispersion corrections were applied neither in the energy nor in the pressure. In the simulations of the protein in solution the coupling was applied isotropically, while in the simulations in the presence of the membrane the pressure scaling was applied semi-isotropically, coupling the x and y directions (the membrane plane). The bonds in the protein and the lipids were constrained using the LINCS algorithm [31]. For the bonds and bond-angle of the water molecules we used the SETTLE algorithm [32]. The time step for the integration of the equation of motion was 5 fs due to the use of virtual sites in the polar hydrogen atoms of the protein and lipids [33]. The non-bonded list was updated every 4 steps. To release initial steric clashes we performed 1000 steepest descent cycles. Prior to every production run, a equilibration step of 1 ns was performed applying position restraints to the backbone atoms in the protein. The restraint forces were 1000, 600, 200, and 75 kJ/Å^2 in each equilibration step respectively. Every run, whether of equilibration or production, was started with a different set of initial velocities in order to produce different trajectories. The simulations in high ionic strength were equilibrated for another 15 ns. Production runs were performed without restrictions during 100 ns. The simulations and most of the analysis were done with the GROMACS 4.0 software package [34].

The PMF was calculated by using the constraint pull code algorithm implemented in GROMACS. A constraint between the centers of mass of the *cis* hemilayer (the hemilayer closest to the protein), and the protein.

The pull rate was set to 0.00 nm/ps to make a static-equilibrium treatment of the problem. The forces in Fig. 6A are the forces of the constraint required to keep constant the distance between the two centers of mass.

2.6. Potential of mean force calculations

Eight frames generated in the free molecular dynamics corresponding to different distances from the membrane were used as starting points for simulations. A force was applied between the protein center of mass (CM) and the CM of the phosphorus atoms in one hemilayer to keep a constant distance between the protein and the membrane (center of mass pulling method, in GROMACS). The force was recorded in each simulation step. Runs of 100 ns were performed for each fixed distance, and the force was averaged over each simulation. The set up and pre-equilibration were as in the free molecular dynamics. The distance constraint was also applied in the equilibration stage. The mean force was integrated along the normal distance to the membrane. The error was estimated by block averaging over the trace [27]. It was verified that the simulations were long enough to produce significant differences among the different systems. For the constrained simulations, the size of the box in the direction normal to the membrane was 13 nm. The concentration of NaCl in the high ionic strength condition was 0.5 M. Electric field along the z axis was evaluated by double integration of the charge density with the algorithm included in GROMACS. The secondary structure content of the protein was analyzed using the DSSP program of Kabsh and Sander [35].

3. Results

3.1. Binding of ReP1-NCXSQ to phospholipid membranes. Filtration assay

Fig. 3 shows the fraction of ReP1-NCXSQ bound to lipid membranes as a function of the total amount of lipid. Binding was stronger to the anionic membranes of POPG in the medium of low ionic strength (0.01 M NaCl). Increasing the ionic strength to 0.1 M NaCl or using the

zwitterionic lipid POPC, produced a large decrease in protein binding. These observations indicate that electrostatic interactions are a major driving force for the binding of ReP1-NCXSQ to the lipid membrane.

3.2. Unconstrained molecular dynamics. Simulations of the spontaneous adsorption

Considering that ReP1-NCXSQ binds to the anionic lipid POPG and that the binding is decreased in high ionic strength and in zwitterionic lipids, we simulated these three different systems: ReP1-NCXSQ in the presence of anionic lipid membranes of POPG, in low and high ionic strength, and ReP1-NCXSQ in the presence of POPC lipid membranes in low ionic strength. We performed three runs for POPG in low ionic strength, two runs for POPG in high ionic strength and two runs for POPC.

For each run, in the three membrane systems, first we performed simulations of 50 ns with the protein restrained at the initial distance and orientation. The average lipid area in all cases remained constant during these equilibrations and also during the next 100 ns of production runs.

The simulations started with ReP1-NCXSQ in the aqueous phase with the CM at about 3.5 to 2.5 nm from the plane of phosphorus atoms in the membrane (the membrane plane). This gap was equivalent to about 10 to 7 layers of solvent. Fig. 2 shows representative frames at the beginning (Fig. 2A, B and C) and the corresponding frames at the end of the simulations (Fig. 2D, E and F) for the system ReP1-NCXSQ-POPG at low ionic strength. The magnitude and orientation of the protein macrodipole, shown in Fig. 1C and Fig. 2, were relevant to explain the binding and orientations of ReP1-NCXSQ within the membrane environments as we will describe below. The main contribution to the dipole was from the partial and net charges of the amino acid sidechains. The average magnitude was 350 Debyes with a fluctuation of ±50 Debyes. The orientation of the dipole within the protein backbone frame was practically constant. Therefore, it was used to describe the orientation of the whole molecule. For comparison, we evaluated the macrodipole of other representative proteins that bind peripherally to lipid membranes and for which their orientation within the interface were studied. The calculated dipole of proteinase 3 was 412 Debyes [8], for the intestinal fatty acid-binding protein 385 Debyes [4], for phospholipase A2 320 Debyes [9] and for liver bile acid binding protein it was 175 Debyes [14]. The macrodipole of ReP1-NCXSQ is about the same size as the macrodipoles of peripheral proteins with affinity for
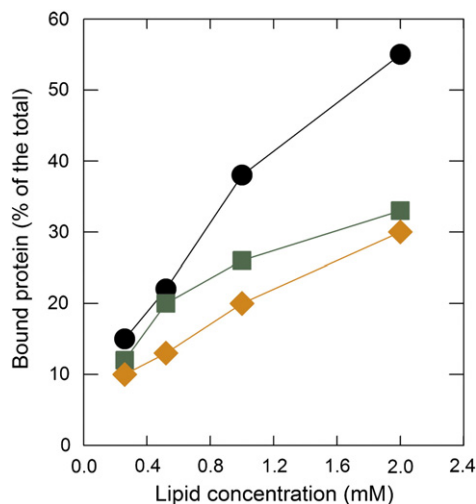
anionic membranes. The relevance of the dipole magnitude was evidenced after evaluating the energy of the interaction with the membrane electric field, as described in a following section. The net charge on the protein $Z = -1$ was maintained constant through the simulations.

Fig. 4 shows the distance between the protein CM and the membrane plane (Fig. 4, left column), and the angle determined by the electric macrodipole of the protein and the membrane plane (Fig. 4, right column) along the different trajectories. Zero degree corresponds to the dipole parallel to the membrane plane and 90 or −90° to a normal orientation. Positive values correspond to the positive end pointing towards the membrane. All distances and angles are relative to the lipid hemilayer closer to the protein, this is the cis hemilayer.

3.2.1. Interactions with anionic lipids at low ionic strength

Fig. 4A shows that the CM of ReP1-NCXSQ approached to the membrane and reached a location at a constant distance of about 1–1.5 nm depending on the simulation. The protein reached orientations in which the macrodipole was preferentially oriented with the positive end pointing to the anionic interface with angles of about +44, +54 and +60°, in the three simulations (Fig. 4B). Even when the dipole was initially aligned in the opposite direction (red trace, starting at −50° in Fig. 4B), the protein rotated until the dipole was pointing to the negative surface. At 20 ns, corresponding to a distance of 1.5–2 nm, ReP1-NCXSQ was oriented with the dipole even more perpendicular to the membrane plane, this is with an angle of 60–70 positive degrees (black, red and blue traces in Fig. 4B).

3.2.2. Interactions with anionic lipids at high ionic strength

The green and pale blue traces in Fig. 4C show that in the presence of high ionic strength the approach of the protein to the membrane was slower than in low ionic strength. The final distance was also larger. The largest angle sampled was of +70° and it was reached at the same average distance as in low ionic strength, at about 2 nm. It is remarkable that at intermediate distances (2–3 nm) or times (20–50 ns) the protein explored orientations with negative values for the angle between the dipole and the normal to the membrane (Fig. 4D). We conclude that the effect of the membrane electric field on the orientation was shielded by the presence of the soluble ions. Longer time was required to reach the final orientation. Still, this was similar to the orientation observed in the absence of NaCl.

3.2.3. Interactions with zwitterionic lipids

A distinguishable difference with the anionic lipid was that the final orientation was rather parallel to the membrane plane, with the dipole in an angle of 25° in one simulation and in a completely different orientation with the dipole pointing to the aqueous phase (angle of −75°) in the other (Fig. 4F).

Fig. 5 shows the frequency distribution of distances and orientations for all the systems. The frequencies were evaluated along the last 30–40 ns of simulations. In agreement with previous descriptions, the general trend was that the distances to the membrane were shorter for the POPG at low ionic strength systems (red, black and blue traces). In the POPG, high ionic strength systems, the distribution peaks were located at longer distances (green and pale blue traces in panel A). Regarding the orientations, all the distributions for the POPG systems, both at high or low ionic strength, were located within the range of 40–70 positive degrees.

3.3. PMF calculation using constrained simulations: differential selectivity of ReP1-NCXSQ towards different lipid membranes

Fig. 6A shows the mean forces at different distances (see Material and methods section for PMF calculations). At the largest distance, when the protein was in the bulk water, the force was zero in all simulations. In agreement with the migrations observed in the spontaneous

Fig. 3. Binding of ReP1-NCXSQ to LUVs. The fraction of the total protein bound to the lipid membrane is plotted as a function of the total amount of lipid (see Materials and methods section, binding assay). LUVs of (●) POPG in 0.01 M NaCl, (■) POPG in 0.1 M NaCl, (◆) POPC in 0.01 M NaCl. Samples contained 5 μM protein, pH was 6.7. Temperature was 22 °C.
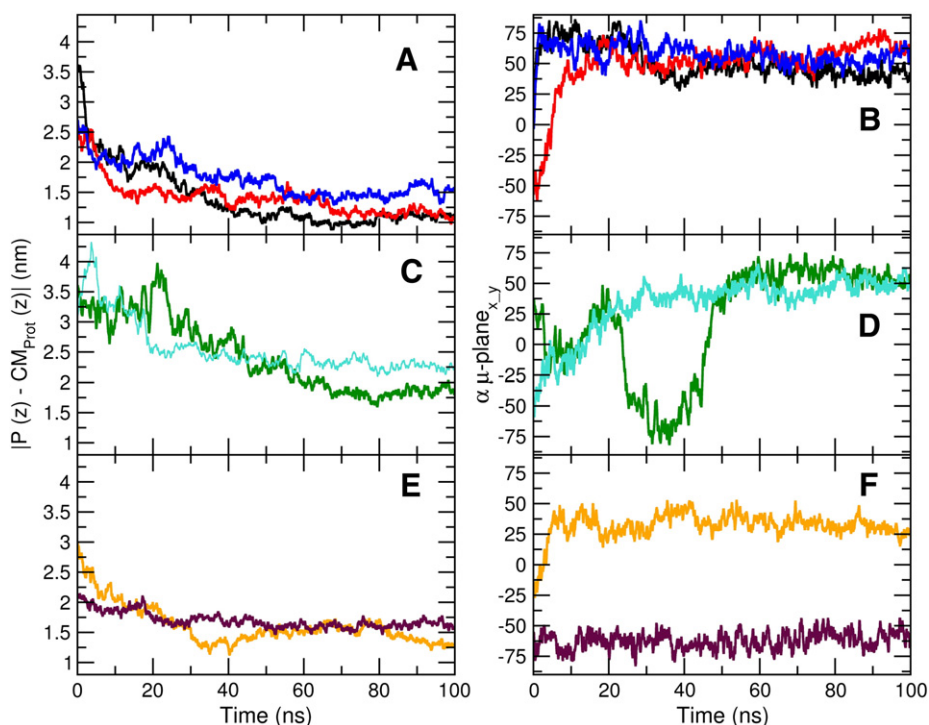
Fig. 4. Trajectory of the unconstrained molecular dynamics of ReP1-NCXSQ with POPG and POPC membranes. Left column: the distance between the protein center of mass and the average plane of phosphorus atoms of lipids. Right column: the angle between the protein electric macrodipole and the average plane of phosphorus atoms in the membrane. A and B: POPG membrane in low ionic strength. C and D POPG in 1 M NaCl. E and F: POPC membrane in low ionic strength. Traces correspond to separate simulations.

adsorptions (Fig. 4), an attractive (positive) force was observed at shorter distances. In the systems containing POPG, the general trend was that the forces in the simulations at high ionic strength were weaker than at low ionic strength. Nevertheless, at distances shorter than 1.25 nm both systems converged to about the same value. This can be explained considering that when the protein is far from the membrane, the ions in between can shield the membrane electric field in the high ionic strength system. In the POPC system, net attractive forces were also observed, but in this case they appeared only at distances shorter than 3 nm. We highlight the fact that the forces in POPC appeared at

shorter distances, while in POPG seem to be of longer range. At 2.5 nm, for POPC, the fluctuation in the magnitude of the force was quite large (se error bar in Fig. 6).

Fig. 6B shows the PMF obtained by numerical integration of the mean forces over the protein CM-membrane distance. The PMF calculated in this way is a good approximation to the reversible work for transporting the protein from the bulk solution up to a given distance to the membrane and can be considered as the free energy of the process [36–38]. To have a reference, the values that we obtained were in the same order as those obtained for the interactions of the amyloid-β
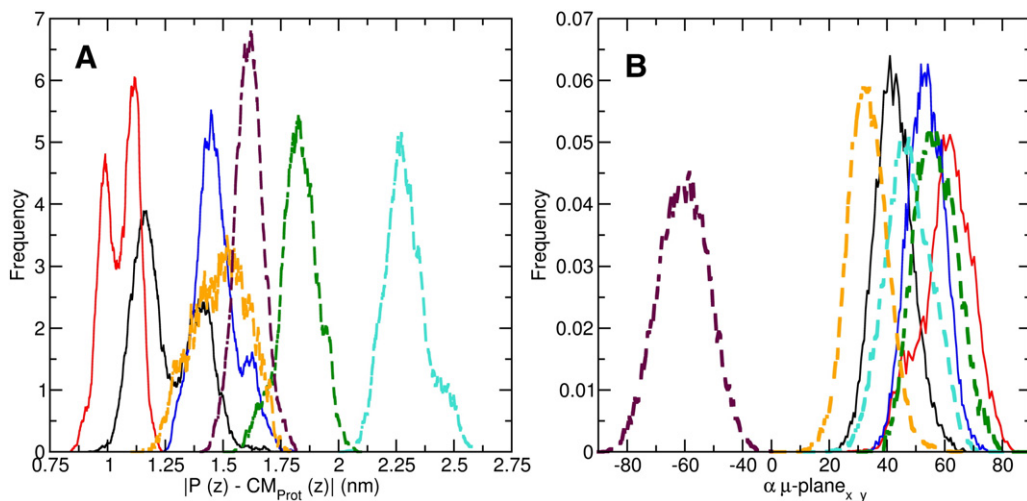

Fig. 5. The distribution of distances and orientations. A: the frequency of distances between the protein center of mass and the average plane of phosphorus atoms in the lipids. Colors correspond with the traces in Fig. 4. Distributions were centered at: POPG low ionic strength double peak at 0.9 and 1.1 nm (red), double peak a 1.12 and 1.3 nm (black) and 1.35 nm (blue); POPG 1 M NaCl 2.25 nm (pale blue) and 1.8 nm (green); POPC low ionic strength 1.6 nm (violet) and 1.5 (orange). B: the frequency of angles between the protein macrodipole and the average plane of phosphorus atoms in the lipids. Colors correspond with the traces in Fig. 4. Distributions were centered at: POPG low ionic 65° (red), 40° (black) 50° (blue); POPG 1 M NaCl 45° (pale blue) 55° (green); POPC low ionic strength −60° (violet) and 35° (orange).

Fig. 7. Orientation of ReP1-NCXSQ in the constrained simulations. The average angle between the protein macrodipole and the plane of the membrane. Error bars are the standard deviation of the distribution. (●) membrane of POPG in low ionic strength; (■) membrane of POPG in the presence of 0.5 M NaCl; (♦) membrane of POPC in low ionic strength; (○) the average angle between the macrodipole and the *x*–*y* plane in a simulation in solution, without lipid membrane; its location in the plot is not related to the distance axis. Error bars are the standard deviation of the distributions.
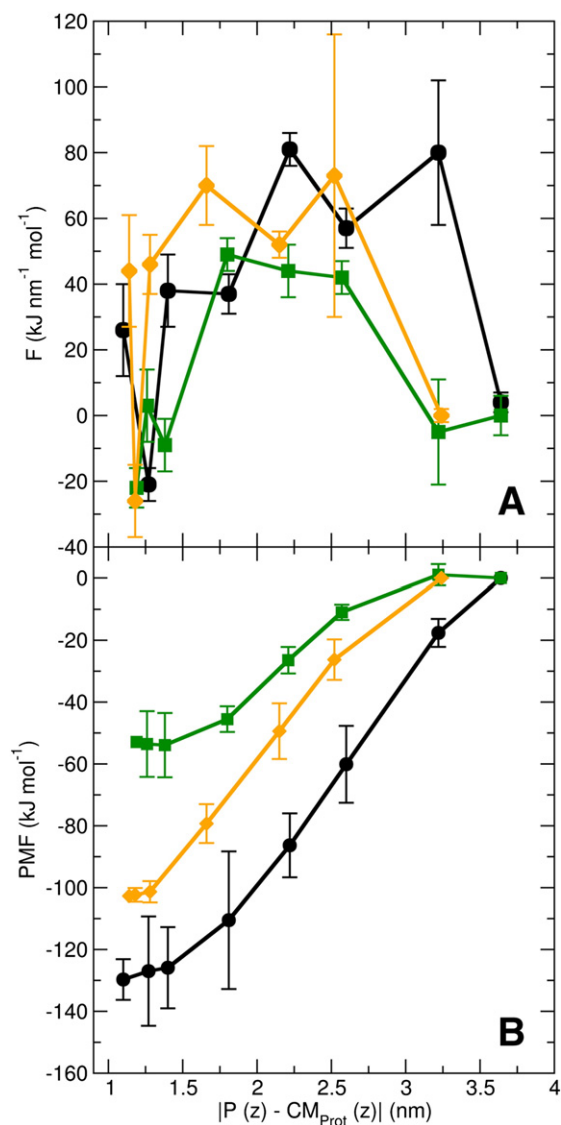

Fig. 6. Constrained MD. Mean force and PMF. A: The average mean force between ReP1-NCXSQ center of mass and the closest hemilayer evaluated in the constrained molecular dynamics at the fixed distances. B: potential of mean force calculated by integration of the forces in panel A. Bars indicate the error estimated by block averaging over the trace. (●) membrane of POPG in low ionic strength; (■) membrane of POPG in the presence of 0.5 M NaCl; (♦) membrane of POPC in low ionic strength.

peptide with anionic lipid membranes [39]. Fig. 6B shows that the binding to POPG in low ionic strength occurred with the largest negative ΔG at all distances. In agreement with the experimental results, the increase in NaCl concentration produced a decrease in the binding free energy. The binding to the zwitterionic lipids was also less favorable than to POPG at low ionic strength.

3.4. Orientation of ReP1-NCXSQ from constrained simulations

We evaluated the orientation of the protein also in the distance-constrained simulations. The average orientation of the macrodipole is shown in Fig. 7. The first observation was that the membrane induced a decrease in the rotational mobility of ReP1-NCXSQ even at a distance at which the net attractive force was zero: In 100 ns of simulation in solution, in the absence of a membrane, the average angle between the protein macrodipole and any of the axes, was about zero with an standard deviation of 40° (see the separate point in Fig. 7). This strongly suggests that in the absence of the membrane the protein was able to sample the whole rotational space in solution. The comparison with
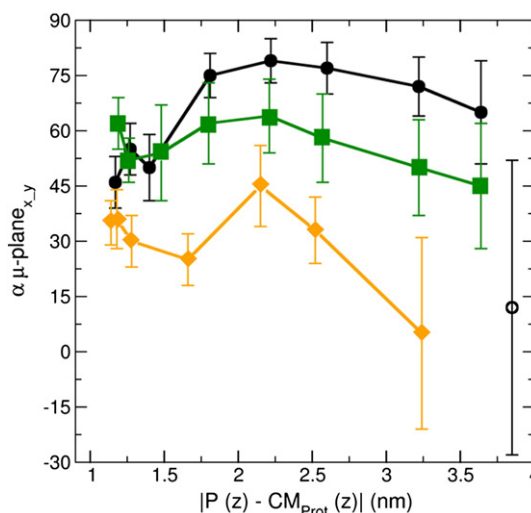
the simulations in the presence of membrane clearly indicated the effect of the membrane in restricting the rotation and inducing a preferred orientation: In POPG in low ionic strength, ReP1-NCXSQ was oriented with the dipole almost perpendicular to the membrane plane, acquiring an angle of about +76°, when it was between 1.7 and 2.5 nm from the membrane. The angle was biased towards a more parallel orientation at shorter distances. A similar profile was obtained in the presence of high ionic strength but a smaller angle of +60° was reached. The error bars in Fig. 6 are the standard deviation of the distribution, they are a measure of fluctuations in the orientation and indicate that in the presence of high ionic strength ReP1-NCXSQ explored a higher number of orientations as compared with the system containing low ionic strength. At short distances, below 2 nm, both systems were biased to a more parallel orientation. It can be concluded that the shielding of the electrostatic interactions with anionic membranes increased when electrolytes were able to fill the space between the protein and the membrane. In zwitterionic membranes, the average orientation at long distances was parallel to the plane of the membrane and the number of explored orientations was even larger than in POPG in 0.5 M NaCl. This was evidenced by the larger error bar in the point at 3.25 nm. In all cases, the fluctuations in the orientations decreased at shorter distances. This effect could be due to the local contacts and hydrogen bond interactions with the lipid polar head groups as described below.

The electrostatic energy of a dipole in an electric field is $U^e = \mathbf{p} \cdot \mathbf{E}$. Where $\mathbf{p}$ is the dipole moment vector and $\mathbf{E}$ the electric field vector. The distribution of dipoles oriented antiparallel and parallel to the electric field, in the absence of other restrictions, is $Na/Np = \mathrm{EXP}(\Delta U^e_{\mathrm{a-p}}/k_{\mathrm{B}}T)$. Na and Np are the number of protein molecules in antiparallel and parallel orientations, respectively. $\Delta U^e_{\mathrm{a-p}}$ is the energy difference between these configurations. k_{B} and T are the Boltzmann constant and the absolute temperature. We evaluated the electrostatic potential for different distances along z axis, by double integration of the charge density. From the derivative of the electrostatic potential with the distance we also evaluated the electric field. Fig. 8 shows the electrostatic potential (panel A) and the electric field (panels B and C) as a function of the distance to the plane of phosphorus atoms of the membrane. We obtained a value of 3×10^7 V m^{-1} for the electric field at a distance between 1.5 and 2 nm. For an electric field of 3×10^7 V m^{-1} (0.03 V nm^{-1} in Fig. 8C) and a dipole of 380 Debyes, the energy difference between the parallel and antiparallel orientation is 3.81×10^{-20} J, which is about
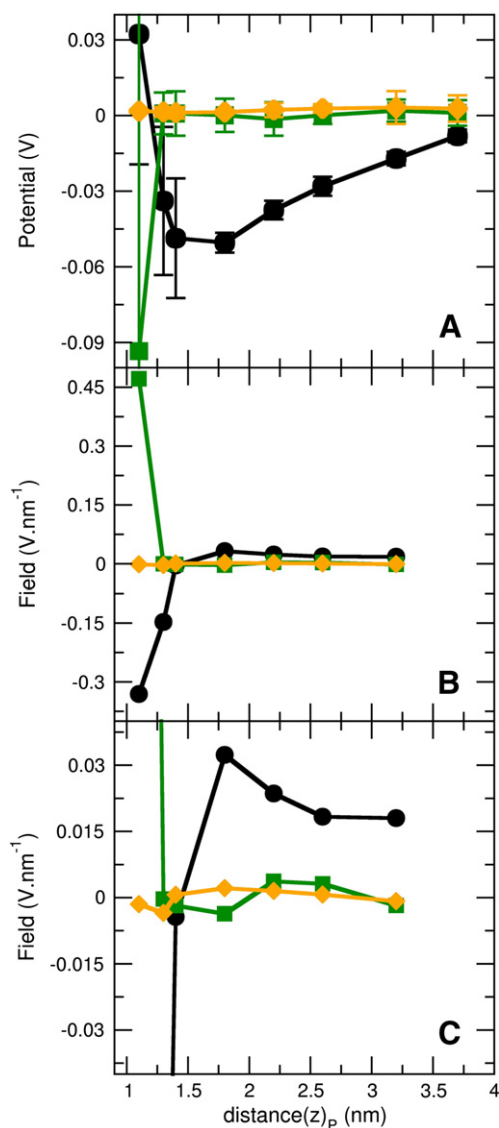
Fig. 8. Electrostatic surface potential and electric field. A: the electrostatic potential as a function of the distance to the average plane of phosphorus atoms in the lipids calculated by double integral of the charge density. B: electrostatic field calculated as the distance derivative of the electric field. C: Enlarged scale of panel B. (●) POPG in low ionic strength; (■) POPG in 1 M NaCl; (◆) POPC in low ionic strength.

eight times the value of k_BT at 320 K (0.441×10^{-20} J). Then, the fraction of molecules with the dipole oriented antiparallel to the electric field, this is in the higher energy configuration, is 1.8×10^{-4}. We conclude that the difference of electrostatic energy between the parallel and antiparallel orientation of the dipole in the membrane electric field is within the range required to produce a bias towards a preferred orientation.

At a shorter distance, below 1.5 nm, the electrostatic potential decreased and reached even a positive value (Fig. 8A). The electric field changed its orientation and reached a larger value of -0.2×10^9 V m^{-1}. According to this electrostatic potential and electric field landscape, ReP1-NCXSQ should acquire an opposite orientation at shorter distances. This radical change in the orientation was not observed in the simulations. It must be noted that the electric field changed within a distance range comparable to the size of the protein. At this point we are not allowed to consider a simple model of field–dipole interaction to predict which should be the orientation, because different regions of the protein, which contribute to the macrodipole, are "feeling" very different values for the field. Besides, local interactions also define the orientation of the protein in the

interface. Fig. 8 (panels B and C) also shows that the electric field produced by POPG membranes in the presence of high ionic strength and by the zwitterionic lipid POPC was negligible at long distances. This can account for the lower degree of orientation within these interfaces at long distances.

The attractive force in the POPG low ionic strength system could be attributed to the interactions of negative surface potential with positive charges in the protein closer to the membrane. Nevertheless, Fig. 8 shows that the potential in the presence of high ionic strength or in the zwitterionic membranes is much smaller or even negligible. This requires further explanation for the appearance of the force in these systems. As explained before, the forces were zero at long distances for POPG high ionic strength and POPC. They were different from zero at distances at which a small number of transient contacts were available. Simple diffusion to any of the hemilayers in the periodic cell could drive an approach that results in the appearance of a net attractive force due to transient contacts.

3.5. Evaluating the changes in the lipid order and in the protein conformation

To evaluate possible global changes in the structure of the systems due to lipid–protein interactions, we measured the average area of the lipids in the membrane and the number of residues participating in secondary structure in the protein. To evaluate these parameters we used the ensembles of conformations generated in the distance constrained simulations. Fig. 9A shows that the average lipid area remained constant for the three systems along the simulations and within the cannonical values for phospholipids in a bilayer. For each run, in the three membrane systems, first we performed simulations of 50 ns with the protein restrained at the initial distance and orientation. The average lipid area in all cases remained constant during these equilibrations and also during the next 100 ns of production runs. The values for the lipid average areas were (0.70 ± 0.01) nm^2, (0.69 ± 0.01) nm^2 and (0.69 ± 0.01) nm^2 for POPG in absence and in presence of NaCl and POPC respectively. The value for POPC was in agreement with the obtained experimentally by Kucerka et al. of 0.68 nm^2 [40] but larger than the value of 0.65 nm^2 evaluated by MD simulations by Dickey and Faller [41]. Our values for POPG were about 27% larger than the areas obtained by Dickey and Faller [41] but only 6% larger than the experimental value of 0.66 nm2 obtained by Kucerka et al. [42]. We did not further explore the basis of this difference. Besides, we performed simulations of 400 ns in the absence of protein for POPG in the presence and in the absence of NaCl and for POPC. These systems reached the same average areas of 0.7 nm^2. Despite the difference in lipid area for POPG with other simulations, our systems were converged with respect to the lipid organization and this organization did not change because of the interaction with the protein.

After 100 ns of simulation in solution, in the absence of membrane, the C_α carbons average RMSD from the crystallographic structure reached a convergent value of 0.19 ± 0.02 nm. This indicated that the protein remained well within the crystallographic structure. As a reference, it can be considered that the molten globule state of α-lactalbumin, reaches a RMSD > 1 nm from the crystallographic structure [43]. Fig. 9B shows the average RMSD, from the average structure simulated in solution, for the distance constrained simulations. At all distances, the RMSD values corresponded to a protein that was not distorted and remained within the native structure. Still, it can be observed in all systems a tendency to unfold at an intermediate distance from the membrane between 2.5 and 3 nm.

Fig. 9C shows that the average number of residues with defined secondary structure, according to the criteria of Kabsch and Sander [35], remained essentially constant along the distance to the membrane in the different systems. The constancy of this number does not necessarily mean constancy in the protein conformation: some residues could shift from strands to helical conformation, keeping the amount
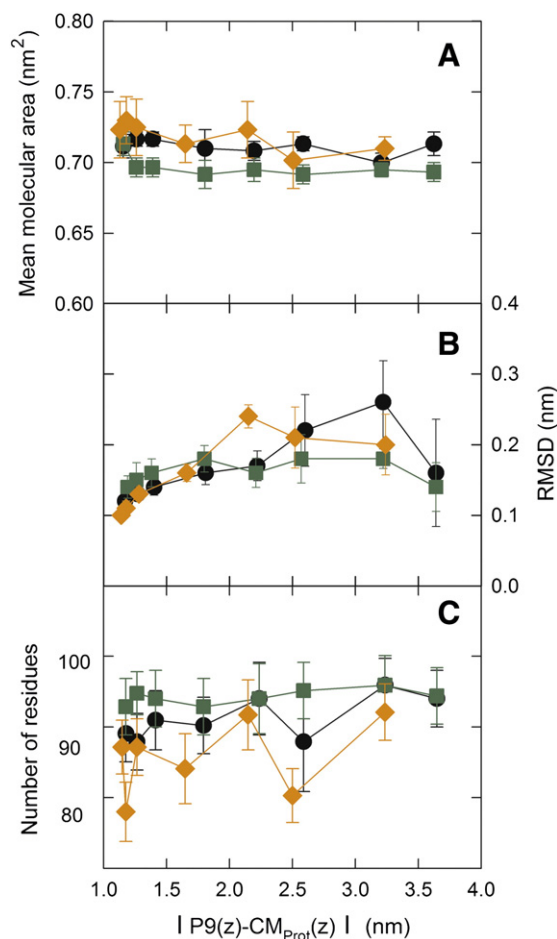
Fig. 9. The lipid organization and protein conformation. A) The lipid mean molecular area as a function of the membrane-protein distance B) Average C_α RMSD from the average structure in solution, in the absence of the membrane. C) The number of amino acids involved in secondary structure as a function of the membrane-protein distance. (●) POPG in low ionic strength; (■) POPG in 0.5 M NaCl; (◆) POPC in low ionic strength. Error bars are the standard deviation for each distribution.

of secondary structure constant, for example. Instead, visual inspection and RMSD values revealed no changes in the protein conformation. We were not able to identify a particular region undergoing conformational changes. The figure shows that the numbers for the system containing POPC were lower than for the other systems. Being the global conformation constant, this observation suggest that in this system the structure was more fluctuating, with more residues along the whole chain temporarily exchanging between the on-off state of intramolecular hydrogen bonds that define the presence of secondary structure.

A relevant observation, useful for the interpretation of the main results in this work, is that the small fluctuations in secondary structure, revealed by the error bars in the figure, were not translated into major changes in the magnitude an orientation of the protein macrodipole.

3.6. The details of ReP1-NCXSQ–lipid interactions. Protein–lipid contacts and hydrogen bonds

We evaluated the contacts between protein and membranes in the configuration of lowest free energy obtained in the PMF, when the CM of ReP1-NCXSQ was at 1.2 nm from the plane of the membrane. We defined a contact when an atom in the protein was at a distance equal or lower than 0.6 nm from an atom that belongs to a lipid. For this cutoff, at most one molecule of solvent can be located between the groups. If we chose a smaller cutoff, almost no contacts were observed for the POPC system. Then, to have a value to compare with, we decided to use this rather long cutoff distance and to evaluate how the number

of contacts were increased in the POPG systems. Fig. 10 shows the number of contacts that any atom in the indicated residue made with any atom belonging to a lipid. Data are the average number of contacts per frame evaluated along the converged portion (the last 30–40 ns) of the dynamics. Actually, a larger number of residues made contacts with the membrane. For the analysis, we considered, and included in Fig. 10, only the contacts for which the standard deviation was smaller than the average value and then could be considered more stable contacts. Fig. 11 shows the residues that made contacts with lipids. In the anionic membrane, low ionic strength, the amino acids that made stable contacts were Met28, Val29, Lys32, Phe58, Thr60 and Lys80, located in the α-helix domain or very close to it, and Lys8 and Lys53 located on one side of the β-barrel. Note that Lys8 is located next to the bottom of the barrel.

In the presence of high ionic strength, the set of residues that made contacts with the membrane were Asp18, Asp19, Lys22, Glu25, Arg31, Asn35, Met28 and Lys32 located in the α-helix domain and Arg79, Lys80 and Thr57 in β-turns very close to the α-helix domain. No residues from the barrel, far from the helix domain, made contacts (Fig. 11).

In the zwitterionic membrane a different set of residues established contacts with the membrane: Val24, Gly27, Met30 and Lys32 located in the α-helix domain and Thr60, Lys82 and Thr60 located in the β-barrel.

We also evaluated the presence of hydrogen bonds (HBs) between protein and lipids. An HB was defined when the distance between donor and acceptor atom was shorter than 0.35 nm and the angle determined by donor-H-acceptor was lower than 30°. The number of HBs was evaluated as a temporal average. The counting was done in the same set of frames used to evaluate the number of contacts. Among the set of amino acids that made contacts in the POPG, low ionic strength system, we found that Lys8, Lys32, Lys53 and Lys80 made HBs with lipids. In the anionic membrane with high ionic strength Arg31, Arg79 and Lys 80 made HBs with the lipids. No stable HBs were observed in zwitterionic membrane system.

In the low ionic strength system, we included 129 Na$^+$, while in the high ionic strength system they were 297 Na$^+$ and 168 Cl$^-$. In the systems containing the anionic lipid POPG, we evaluated the number of contacts between Na$^+$ ions and lipids within a layer of 0.3 nm thick and within a layer of 0.6 nm from the membrane plane, corresponding to one and two hydration layer. The count was made separately for the two lipid hemilayers. In the low ionic strength system we found 11 and 80 contacts between Na$^+$ ions and lipids considering one or two hydration layers respectively. In the system with 0.5 M NaCl, were 11 and 90 contacts. When the protein was bound, no change in the number of Na$^+$–lipid contacts were observed in the system with low ionic
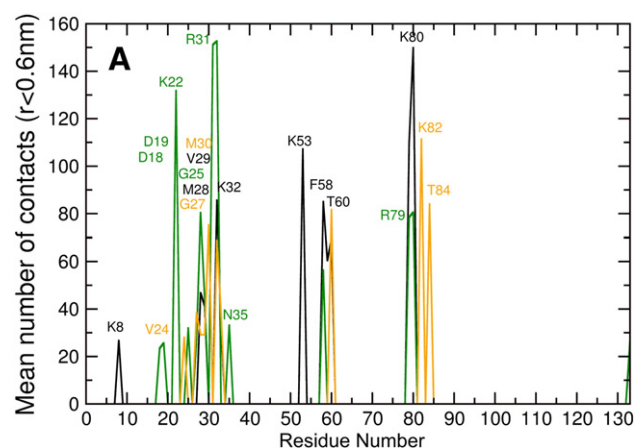

Fig. 10. Contacts between ReP1-NCXSQ and the membrane. Frequency of contacts between the residues in ReP1-NCXSQ and lipids. Data were from constrained simulations (calculation of PMF) with the protein center of mass at 1.4 nm. Black: POPG in low ionic strength; green: POPG in presence of 0.5 M NaCl; orange: membrane of POPC in low ionic strength.
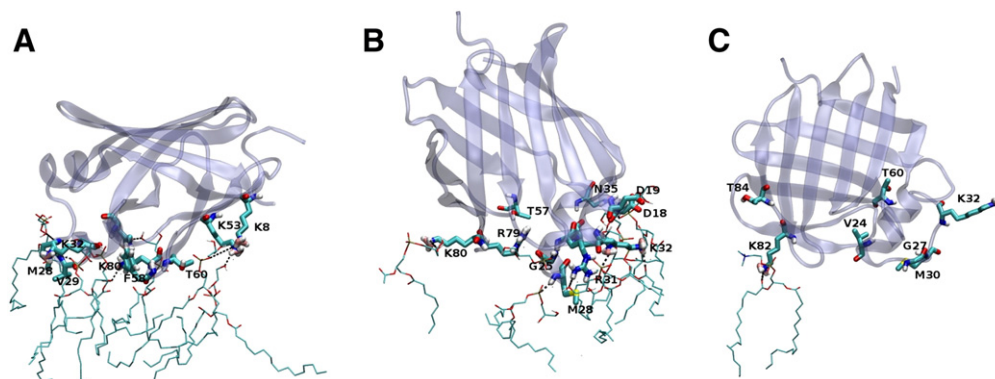
Fig. 11. The residues that make contacts with lipids. A: membrane of POPG in low ionic strength; B: membrane of POPG in 0.5 M NaCl; C: membrane of POPC in low ionic strength. Hydrogen bonds are shown in dashed lines.

strength. Instead, in the system containing 0.5 M NaCl, 10 contacts between Na$^+$ and lipids were removed but only if we considered the thicker hydration layer.

4. Discussion

In the unconstrained dynamics, the protein CM reached an invariant distance to the lipid membrane at 1–1.5 nm from the plane of phosphate groups. This is the same distance at which the free energy, evaluated from the constrained dynamics, reached a constant, large negative value.

According to the filtration assays and to the PMF calculation, the binding was stronger to the anionic interfaces in low ionic strength. Increasing NaCl concentration or replacing the anionic by zwitterionic lipids produced a decrease in the strength of binding, suggesting that electrostatics is a major driving force, like the general case in which a positively charged protein binds to the anionic lipid membrane. Nevertheless, the binding to the anionic interface, the reduction of the strength of binding by increasing the ionic strength or by using a zwitterionic lipid was observed in the simulations with a protein bearing a net *negative* charge. Together with the capacity of the protein to react and orient within the membrane electric field, this observation strongly suggests that the anisotropic distribution of charges is the relevant factor to determine the binding to the charged interface. At long distances, when the protein was not establishing contacts with the lipids, it acquired an orientation determined by the interactions of the macrodipole with the electric field generated by the net charges in the membrane (POPG at low ionic strength). Such orientation allowed the partial positive density of charges (positive end of the macrodipole) to be closer and more available to the anionic lipids. This picture fits within a simple electrostatic model for a dipole in the homogeneous field produced by a plane of charges. Closer to the membrane, also local interactions such as specific electrostatics (hydrogen bonds, dipolar interactions, salt bridges) or Van der Waals interactions, could be established with the lipids and became more relevant than the long range electrostatics to determine the final orientation. The role of the electric field on the protein orientation is even more evident when we consider that at middle and long range distances, the zwitterionic POPC membranes did not produce a preferential orientation of ReP1-NCXSQ as evidenced by the larger distribution of orientations.

According to unconstrained simulations, ReP1-NCXSQ binds peripherally and does not penetrate into the hydrophobic core. The dependence of the strength of binding with the surface charge and ionic strength is also consistent with peripheral, electrostatic interactions.

In several systems, clusters or domains of positively charged residues in the protein have been described to drive the interaction with anionic lipids in the membrane. The MARCKS protein has a cluster of Lys residues in the primary sequence making a binding domain with affinity for anionic lipids [3]. Cytochrome *c* also binds to anionic

membranes by electrostatic interactions; labeling experiments have shown that the binding domain is composed by a cluster of Lys residues [10]. In the case of ReP1-NCXSQ, the positively charged residues that made contacts with the membrane were not identified as a separate cluster from other residues. In other words, the observation of the whole set of Lys and Arg residues gave no clue (considering the clustering in the primary or tertiary structure) about the location of the binding site. Only the global evaluation of the protein dipole or electrostatic potential gives a clue about the orientation that the protein will acquire in the interface. Still, this information is not enough to predict the final orientation for the bound state: at short distances between protein and membrane, local interactions become relevant and can bias the orientation dictated by simple alignment of the protein dipole with the membrane electric field.

We evaluated the protein macrodipole in several systems where the orientation within the membrane environment of the peripheral proteins is available [4,8,9,14]. In all cases we observed that the magnitude of the macrodipole was about the same size of the dipole of ReP1-NCXSQ. Besides, the positive end was also pointing towards the anionic lipid membrane. As already shown by Zamarreño et al. [15], the orientation of proteins in the interface is strongly biased by the interaction of the macrodipole with the membrane electric field. In the present simulations, this was actually demonstrated within a space region where the rotation was not impaired by contact interactions: at 2.5 nm the evaluation of dipole–field interaction energy indicated that the parallel orientation must be preferred. As in the simulation of proteinase 3, for example [8], the preferred orientation in our case was one of the emergent results of the simulation. The orientation was actually parallel both in the unconstrained and in the distance-constrained simulations at this distance. Nevertheless, at shorter distance, to consider a point dipole within a uniform electric field is no longer valid. Inspection of the microscopic profile of the field as a function of the distance revealed a puzzling picture: within a very short distance, as compared with the protein dimensions, the electric field changes from a negative value at 2.5 nm to zero at 1.5 nm and to positive values at 1 nm from the plane of the lipid phosphate groups. When the CM was located, for example at 1.5 nm, large portions of the protein were placed at very different values of the electric field. Prediction of the orientation due to the interaction of the field with the microscopic details of the protein was achieved only as result of the simulation. Besides, at short distance, local contacts were established with the lipids, also restricting the orientation. These contacts are a further contribution to the free energy, beside the electrostatics, and are not taken into account in the pure electrostatic model.

The fact that several peripheral proteins acquire an orientation consistent with a simple macroscopic analysis in which a negative surface orients a dipole in a low energy conformation, suggests that a rationale based in a mean field approximation still has an important predictive value.

In a recent work, the binding of a peripheral protein, oxysterol binding protein, was simulated for one microsecond [7]. It was also observed that in the presence of anionic lipid membranes, the protein rotated and reached a defined orientation independently of the starting orientation. According to the evolution of the interaction energy between protein and membrane, it can be concluded that convergence was reached after 200 ns in most of the runs in that work. It must be noted that convergence was reached in one step. That is, large changes occurred within the first portions of the simulations to reach constant values for the energy term. Similarly, although at shorter times, our simulations occurred with a large change in the distance to the membrane or orientation in the first portion of the run to reach a convergence value.

Some mechanisms for the regulatory action of ReP1-NCXSQ were proposed by Berberián et al. [22]. One of them includes the direct interaction of ReP1-NCXSQ with the lipid membrane (particularly with highly negatively charged phosphoinositides) including the remotion of inhibitory lipids from the environment of the transmembrane protein, essentially phosphoinositides. Then, the predictions of how membrane interactions are conducted by electrostatic interactions are useful to understand the possible mechanisms of the preferential interaction with charged anionic lipids. In this study, we used extreme conditions regarding the composition of the experimental membrane systems, i.e. lipid membranes made of pure anionic or pure zwitterionic lipid membranes. These are not necessarily the conditions found in a plasma membrane, but they were used here as a model system to extract and study the essential features of electrostatic interactions. Still, at microscopic level, high local concentrations of anionic lipids could be relevant to determine binding and orientation.

This work also aimed to understand general aspects of the FABPs binding to target membranes and the molecular determinants of their bimodal mechanism of ligand transfer: collisional or diffusional [44,45]. A certain degree of correlation between the mechanism and the protein orientation was described [15]. These proteins are largely distributed among organisms, from invertebrate to superior mammals. The members of the family have low specificity for the ligand and a highly specific distribution among different tissues within the same organism. Their functions are conserved in the same tissue of different organisms [46,47]. This specificity pattern is related to the primary sequence: orthologs are highly conserved, while paralogs are divergent. Although the high sequence diversity aforementioned (sequence identity homology is around 22–73%), the tertiary structure is highly conserved. This is a nice example of how divergent sequences converge in the same folding. We propose that it is within this sequence diversity, which determines the location of charged residues, where the specificity for an interface and transfer mechanism could be codified.

5. Conclusion

Unconstrained MD and PMF calculations, produced a detailed microscopic picture to understand the forces that drive the binding of ReP1-NCXSQ to the lipid membrane. Both the free and constrained dynamics produced the same results regarding the orientation along the binding pathway for the three studied systems. In the simulations, ReP1-NCXSQ was negatively charged and was preferentially bound to negatively charged lipid membranes at low ionic strength. Together with the binding, rotation of the protein within the membrane electric field was observed. We concluded that the global, asymmetric distribution of electric charges, and further established local interactions, determine in this case the binding to the lipid membrane.

Acknowledgements

References

[1] S.G. Taneva, P.J. Patty, B.J. Frisken, R.B. Cornell, CTP:phosphocholine cytidylyltransferase binds anionic phospholipid vesicles in a cross-bridging mode, Biochemistry 44 (2005) 9382–9393.

[2] S. Qin, A.H. Pande, K.N. Nemec, S.A. Tatulian, The N-terminal alpha-helix of pancreatic phospholipase A2 determines productive-mode orientation of the enzyme at the membrane surface, J. Mol. Biol. 344 (2004) 71–89.

[3] S. Tzlil, D. Murray, A. Ben-Shaul, The "electrostatic-switch" mechanism: Monte Carlo study of MARCKS-membrane interaction, Biophys. J. 95 (2008) 1745–1757.

[4] M. Mihajlovic, T. Lazaridis, Modeling fatty acid delivery from intestinal fatty acid binding protein to a membrane, Protein Sci. 16 (2007) 2042–2055.

[5] M. Pedò, F. Löhr, M. D'Onofrio, M. Assfalg, V. Dötsch, H. Molinari, NMR studies reveal the role of biomembranes in modulating ligand binding and release by intracellular bile acid binding proteins, J. Mol. Biol. 394 (2009) 852–863.

[6] F. Wang, X. Xia, S. Sui, Human apolipoprotein H may have various orientations when attached to lipid layer, Biophys. J. 83 (2002) 985-993.

[7] B. Rogaski, J.B. Klauda, Membrane-binding mechanism of a peripheral membrane protein through microsecond molecular dynamics simulations, J. Mol. Biol. 423 (2012) 847–861.

[8] E. Hajjar, M. Mihajlovic, V. Witko-Sarsat, T. Lazaridis, N. Reuter, Computational prediction of the binding site of proteinase 3 to the plasma membrane, Proteins 71 (2008) 1655–1669.

[9] C.L. Wee, K. Balali-Mood, D. Gavaghan, M.S. Sansom, The interaction of phospholipase A2 with a phospholipid bilayer: coarse-grained molecular dynamics simulations, Biophys. J. 95 (2008) 1649–1657.

[10] C. Kawai, F.M. Prado, G.L. Nunes, P. Di Mascio, A.M. Carmona-Ribeiro, I.L. Nantes, pH-Dependent interaction of cytochrome c with mitochondrial mimetic membranes: the role of an array of positively charged amino acids, J. Biol. Chem. 280 (2005) 34709–34717.

[11] M. Nomikos, A. Mulgrew-Nesbitt, P. Pallavi, G. Mihalyne, I. Zaitseva, K. Swann, F.A. Lai, D. Murray, S. McLaughlin, Binding of phosphoinositide-specific phospholipase C-zeta (PLC-zeta) to phospholipid membranes: potential role of an unstructured cluster of basic residues, J. Biol. Chem. 282 (2007) 16644–16653.

[12] M. Hammel, R. Schwarzenbacher, A. Gries, G.M. Kostner, P. Laggner, R. Prassl, Mechanism of the interaction of beta(2)-glycoprotein I with negatively charged phospholipid membranes, Biochemistry 40 (2001) 14173–14181.

[13] B. Honig, A. Nicholls, Classical electrostatics in biology and chemistry, Science 268 (1995) 1144–1149.

[14] M.A. Villarreal, M. Perduca, H.L. Monaco, G.G. Montich, Binding and interactions of L-BABP to lipid membranes studied by molecular dynamic simulations, Biochim. Biophys. Acta 1778 (2008) 1390–1397.

[15] F. Zamarreño, F.E. Herrera, B. Córsico, M.D. Costabel, Similar structures but different mechanisms: prediction of FABPs-membrane interaction by electrostatic calculation, Biochim. Biophys. Acta 1818 (2012) 1691–1697.

[16] D.F. Vallejo, F. Zamarreño, D.M. Guérin, J.R. Grigera, M.D. Costabel, Prediction of the most favorable configuration in the ACBP-membrane interaction based on electrostatic calculations, Biochim. Biophys. Acta 1788 (2009) 696–700.

[17] M.B. Decca, V.V. Galassi, M. Perduca, H.L. Monaco, G.G. Montich, Influence of the lipid phase state and electrostatic surface potential on the conformations of a peripherally bound membrane protein, J. Phys. Chem. B 114 (2010) 15141–15150.

[18] P.M. De Biase, D. Alvarez Paggi, F. Doctorovich, P. Hildebrandt, D.A. Estrin, D.H. Murgida, M.A. Marti, Molecular basis for the electric field modulation of cytochrome C structure and function, J. Am. Chem. Soc. 131 (2009) 16248–16250.

[19] P. Ojeda-May, M.E. Garcia, Electric field-driven disruption of a native beta-sheet protein conformation and generation of a helix-structure, Biophys. J. 99 (2010) 595–599.

[20] G. Berberián, M. Bollo, G. Montich, G. Roberts, J.A. Degiorgis, R. DiPolo, L. Beaugé, A novel lipid binding protein is a factor required for MgATP stimulation of the squid nerve Na$^+$/Ca^{2+} exchanger, Biochim. Biophys. Acta 1788 (2009) 1255–1262.

[21] D. Raimunda, M. Bollo, L. Beaugé, G. Berberián, Squid nerve Na$^+$/Ca^{2+} exchanger expressed in *Saccharomyces cerevisiae*: up-regulation by a phosphorylated cytosolic protein (ReP1-NCXSQ) is identical to that of native exchanger in situ, Cell Calcium 45 (2009) 499–508.

[22] G. Berberián, A. Podjarny, R. DiPolo, L. Beaugé, Metabolic regulation of the squid nerve Na$^+$/Ca^{2+} exchanger: recent kinetic, biochemical and structural developments, Prog. Biophys. Mol. Biol. 108 (2012) 47–63.

[23] A. Cousido-Siah, D. Ayoub, G. Berberián, M. Bollo, A. Van Dorsselaer, F. Debaene, R. DiPolo, T. Petrova, C. Schulze-Briese, V. Olieric, A. Esteves, A. Mitschler, S. Sanglier-Cianférani, L. Beaugé, A. Podjarny, Structural and functional studies of ReP1-NCXSQ, a protein regulating the squid nerve Na$^+$/Ca^{2+} exchanger, Acta Crystallogr. D Biol. Crystallogr. 68 (2012) 1098-1107.

[24] V. Nolan, M. Perduca, H.L. Monaco, B. Maggio, G.G. Montich, Interactions of chicken liver basic fatty acid-binding protein with lipid membranes, Biochim. Biophys. Acta 1611 (2003) 98–106.

[25] J. Hermans, H.J.C. Berendsen, W.F. van Gunsteren, J.P.M. Postma, A consistent empirical potential for water–protein interactions, Biopolymers 23 (1984) 1513–1518.

[26] A. Kukol, Lipid models for united-atom molecular dynamics simulations of proteins, J. Chem. Theory Comput. 5 (2009) 615–626.

[27] W.F. Van Gunsteren, S.R. Billeter, A.A. Eising, P.H. Hünenberger, P. Krüger, A.E. Mark, W.R.P. Scott, I.G. Tironi, Biomolecular Simulation: The GROMOS96 Manual and User Guide, Zürich, Switzerland, Hochschulverlag AG an der ETH Zürich, 1996.

[28] H. Li, A.D. Robertson, H.J. Jensen, Very fast empirical prediction and rationalization of protein pKa values, Proteins 61 (2005) 704–721.

[29] T. Darden, D. York, L. Pedersen, Particle mesh Ewald: an N-log(N) method for Ewald sums in large systems, J. Chem. Phys. 98 (1993) 10089–10092.

[30] H.J.C. Berendsen, J.P.M. Postma, A. DiNola, J.R. Haak, Molecular dynamics with coupling to an external bath, J. Chem. Phys. 81 (1984) 3684–3690.

[31] B. Hess, H. Bekker, H.J.C. Berendsen, J.G.E.M. Fraaije, LINCS: a linear constraint solver for molecular simulations, J. Comput. Chem. 18 (1997) 1463–1472.

[32] S. Miyamoto, P. Kollman, SETTLE: an analytical version of the SHAKE and RATTLE algorithms for rigid water models, J. Comput. Chem. 13 (1992) 952–962.

[33] K.A. Feenstra, B. Hess, H.J.C. Berendsen, Improving efficiency of large time-scale molecular dynamics simulations of hydrogen-rich systems, J. Comput. Chem. 20 (1999) 786–798.

[34] D. Van Der Spoel, E. Lindahl, B. Hess, G. Groenhof, A.E. Mark, H.J. Berendsen, GROMACS: fast, flexible, and free, J. Comput. Chem. 26 (2005) 1701–1718.

[35] W. Kabsch, C. Sander, Dictionary of protein secondary structure: pattern recognition of hydrogen-bonded and geometrical features, Biopolymers 22 (1983) 2577–2637.

[36] B. Hess, Determining the shear viscosity of model liquids from molecular dynamics simulations, J. Chem. Phys. 116 (2002) 209–218.

[37] Y. Deng, B. Roux, Computations of standard binding free energies with molecular dynamics simulations, J. Phys. Chem. B 113 (2009) 2234–2246.

[38] S. Park, F. Khalili-Araghi, E. Tajkhorshid, K. Schulten, Free energy calculation from steered molecular dynamics simulations using Jarzynski's equality, J. Chem. Phys. 119 (2003) 3559–3567.

[39] C.H. Davis, M.L. Berkowitz, Interaction between amyloid-beta (1–42) peptide and phospholipid bilayers: a molecular dynamics study, Biophys. J. 96 (2009) 785–797.

[40] N. Kucerka, S. Tristram-Nagle, J.F. Nagle, Structure of fully hydrated fluid phase lipid bilayers with monounsaturated chains, J. Membr. Biol. 208 (2005) 193–202.

[41] A. Dickey, R. Faller, Examining the contributions of lipid shape and headgroup charge on bilayer behavior, Biophys. J. 95 (2008) 2636–2646.

[42] N. Kucerka, B.W. Holland, C.G. Gray, B. Tomberli, J. Katsaras, Scattering density profile model of POPG bilayers as determined by molecular dynamics simulations and small-angle neutron and X-ray scattering experiments, J. Phys. Chem. B 116 (2012) 232–239.

[43] N. Bhattacharjee, P. Rani, P. Biswas, Capturing molten globule state of α-lactalbumin through constant pH molecular dynamics simulations, J. Chem. Phys. 138 (2013) 095101.

[44] H.-K. Kim, J. Storch, Mechanism of free fatty acid transfer from rat heart fatty acid-binding protein to phospholipid membranes. Evidence for a collisional process, J. Biol. Chem. 267 (1992) 20051–20056.

[45] J. Storch, A.E.A. Thumser, The fatty acid transport function of fatty acid-binding proteins, Biochim. Biophys. Acta 1486 (2000) 28–44.

[46] L. Makowski, G.S. Hotamisligil, Fatty acid binding proteins—the evolutionary crossroads of inflammatory and metabolic responses, J. Nutr. 134 (2004) 2464S–2468S.

[47] A.W. Zimmerman, J.H. Veerkamp, New insights into the structure and function of fatty acid-binding proteins, Cell. Mol. Life Sci. 59 (2002) 1096–1116.